Narrowing Substrate Specificity in a Directly Evolved Enzyme: The A293D Mutant of Aspartate Aminotransferase[†,‡]

Margaret A. Chow, Kathryn E. McElroy, Kevin D. Corbett, James M. Berger, and Jack F. Kirsch*

Department of Molecular and Cell Biology, University of California, Berkeley, California 94720-3206

Received June 15, 2004; Revised Manuscript Received July 30, 2004

ABSTRACT: Several mutant *Escherichia coli* aspartate aminotransferases (eAATases) have been characterized in the attempt to evolve or rationally redesign the substrate specificity of eAATase into that of *E. coli* tyrosine aminotransferase (eTATase). These include HEX (designed), HEX + A293D (design followed by directed evolution), and SRHEPT (directed evolution). The A293D mutation realized from directed evolution of HEX is here imported into the SRHEPT platform by site-directed mutagenesis, resulting in an enzyme (SRHEPT + A293D) with nearly the same ratio of k_{cat}/K_m^{Phe} to k_{cat}/K_m^{Asp} as that of wild-type eTATase. The A293D substitution is an important specificity determinant; it selectively disfavors interactions with dicarboxylic substrates and inhibitors compared to aromatic ones. Context dependence analysis is generalized to provide quantitative comparisons of a common substitution in two or more different protein scaffolds. High-resolution crystal structures of ligand complexes of HEX + A293D, SRHEPT, and SRHEPT + A293D were determined. We find that in both SRHEPT + A293D and HEX + A293D, the additional mutation holds the Arg 292 side chain away from the active site to allow increased specificity for phenylalanine over aspartate. The resulting movement of Arg 292 allows greater flexibility of the small domain in HEX + A293D. While HEX is always in the closed conformation, HEX + A293D is observed in both the closed and a novel open conformation, allowing for more rapid product release.

Escherichia coli aspartate aminotransferase (eAATase)[1] and tyrosine aminotransferase (eTATase) are paralogs with sequences that are 72% similar and 43% identical. While eAATase readily catalyzes the reversible transamination of dicarboxylic substrates, it effectively discriminates against aromatic substrates (*1*, *2*). In contrast, eTATase is an excellent catalyst for both (*3*).

A major goal of protein engineering is to generate enzymes with targeted specificities. Many efforts that seek to convert the substrate specificity of one enzyme to that of another have been reported (*4*−*8*). Rational redesign and directed evolution have both been used to convert eAATase to an enzyme with specificity approaching that of eTATase.

Homology modeling led to the construction of HEX, an eAATase variant with six mutations based on active site residues conserved in known aspartate aminotransferase sequences but different in eTATase (*9*). The introduced rational substitutions successfully broaden catalytic activity; the specificity of HEX for phenylalanine is increased by more than 3 orders of magnitude, while near-wild-type activity with aspartate is retained. However, HEX does not complement aromatic amino acid auxotrophy in TATase-deficient *E. coli*, and exhibits strong product inhibition as evidenced by low values of K_m and K_D for dicarboxylic ligands (*9*, *10*). A single round of directed evolution of HEX with selection for complementation of tyrosine auxotrophy yielded HEX + A293D,[2] a mutant with *reduced* affinity for dicarboxylic ligands (*10*). A third eAATase variant, SRHEPT, was constructed by combining seven of the most frequently occurring mutations arising from directed evolution of the wild-type enzyme with genetic selection for aromatic aminotransferase activity (*11*). SRHEPT, while exhibiting aromatic and dicarboxylic k_{cat}/K_m values that are comparable with those of HEX, shares only two mutations with it.

A fourth mutant presented here, SRHEPT + A293D, was constructed by introducing the A293D mutation into SRHEPT. Steady-state kinetic parameters were determined for SRHEPT + A293D with phenylalanine, aspartate, and alanine, along with the cosubstrate α-ketoglutarate (α-KG). The new variant has nearly the same specificity for phenylalanine versus aspartate as that exhibited by wild-type eTATase and, in this respect, is a significant improvement over its progenitor, SRHEPT. The effect of the A293D substitution is moderately dependent on the protein scaffold into which it is introduced (HEX or SRHEPT). This conclusion is supported and

[†] This work was supported by NIH Grant GM35393.

[‡] The structures presented in the paper have been submitted to the Protein Data Bank as entries 1TOE (unliganded HEX + A293D), 1TOG (SRHEPT + A293D−Hca), 1TOI (HEX + A293D−Hca), 1TOJ (SRHEPT−Hca), and 1TOK (SRHEPT−maleate).

* To whom correspondence should be addressed. Telephone: (510) 642-6368. Fax: (510) 642-6368. E-mail: jfkirsch@berkeley.edu.

[1] Abbreviations: eAATase, *E. coli* aspartate aminotransferase; eTATase, *E. coli* tyrosine aminotransferase; HEX, eAATase with six amino acid substitutions (V39L/K41Y/T47I/N69L/T109S/N297S); HEX + A293D, HEX with the additional A293D substitution; SRHEPT, eAATase with seven substitutions (A12T/P13T/N34D/T109S/G261A/S285G/N297S); SRHEPT + A293D, variant of SRHEPT with the A293D substitution added; α-KG, α-ketoglutarate; Hca, hydrocinnamate; MDH, malate dehydrogenase; HO-HxoDH, 2-hydroxyisocaproate dehydrogenase; LDH, lactate dehydrogenase; PLP, pyridoxal 5′-phosphate.

[2] Residues are numbered according to the pig cytosolic AATase.

10.1021/bi0487544 CCC: $27.50
Published on Web 09/18/2004

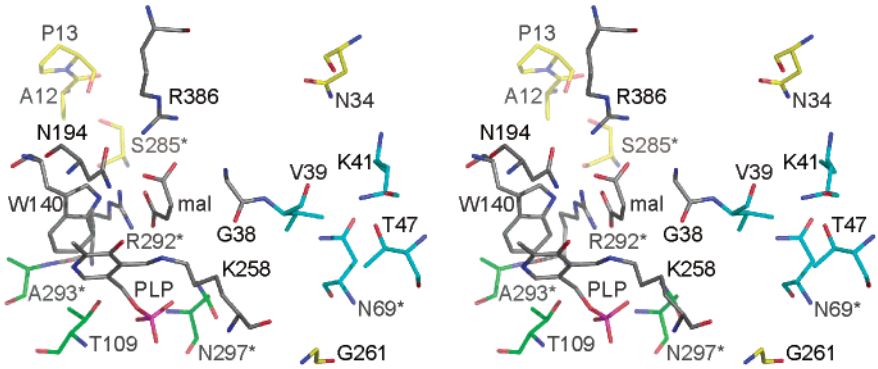

FIGURE 1: Location of HEX and SRHEPT mutations. Stereoview of the wild-type eAATase active site with maleate bound. Residues are colored to indicate the introduced mutations. Gray residues (140, 194, 258, 292, and 386) were not mutated but contact the inhibitor, maleate (labeled "mal"). Cyan residues (39, 41, 47, and 69) are mutated in HEX and HEX + A293D, while yellow residues (12, 13, 34, 261, and 285) are mutated in SRHEPT and SRHEPT + A293D. Two of the green residues (109 and 297) are mutated in all four eAATase variants, and the third green residue (position 293) is mutated in both HEX + A293D and SRHEPT + A293D. Residues marked with an asterisk are contributed by the other subunit.

quantified by the steady-state kinetic data and inhibitor binding assays with maleate and hydrocinnamate (Hca), which are aspartate and phenylalanine analogues, respectively.

High-resolution crystal structures were determined for several complexes of HEX + A293D, SRHEPT, and SRHEPT + A293D. Comparison with the available HEX and eAATase structures gives insight into the mechanisms of manifestation of the mutations. The mutations not only alter direct contacts between the protein and ligand but also promote flexibility of large regions of the enzyme.

EXPERIMENTAL PROCEDURES

Strains and Plasmids. Aminotransferase-deficient *E. coli* strain MG204 (*his*23, *proB*, *trpA-605*, *lacI3*, *lacZ*118, *gyrA*, *rpsL*, Δ*aspC*::*kan*^{r}, *tyrB*, *ilvE*, *recA*::Tn*10*) used for protein overexpression was a gift of I. Fotheringham (Nutrasweet Corp.). *E. coli* strain DH10B (Invitrogen, Carlsbad, CA) was used for plasmid generation. Plasmid pJO2 contains wild-type eAATase downstream of its native promoter in pUC119 (*9*).

Mutants. HEX + A293D and SRHEPT mutants in modified pJO2 are described elsewhere (*10*, *11*). SRHEPT + A293D was derived from SRHEPT by polymerase chain reaction with the mutating primers 5′-GCGGCGATTCGCG-CTAACTACTCTTCCCCACC-3′ and 5′-GGTGGGGAA-GAGTAGTTAGCGCGAATCGCCGC-3′, and external primers and subcloning procedures described previously (*10*). The resulting mutagenic fragments replaced the wild-type sequence in pJO2. Purification of HEX + A293D, SRHEPT, and SRHEPT + A293D followed the protocol of Herold and Kirschner (*12*) with modifications by Onuffer and Kirsch (*9*). Yields were typically ≥100 mg/L, as determined by the absorbance at 280 nm. Figure 1 illustrates the mutations that were made.

Steady-State Kinetics. The concentration of active SRHEPT + A293D was determined from the absorbance at 330 nm following addition of enzyme to 20 mM cysteinesulfinic acid in 200 mM TAPS at pH 8 and 140 mM KCl, where ϵ_{330} = 9140 AU M^{-1} cm^{-1} (*13*). Steady-state kinetics with α-ketoglutarate and aspartate, phenylalanine, or alanine were determined with an MDH, HO-HxoDH (*14*), or LDH coupled assay, respectively, under the conditions described in Table 1. The changes in absorbance at 340 nm arising from the oxidation of NADH by the coupling enzyme were recorded with an Agilent 8453 spectrophotometer. Background rates were measured in the absence of aminotransferase. Data were fit to a straight line with Kaleidagraph (Synergy Software, Reading, PA) for the assay with alanine. For assays with aspartate and phenylalanine, k_{cat} and K_m values were calculated with SAS (SAS Institute, Cary, NC) by a nonlinear regression fit of the data based on eq 1, which describes a ping-pong, bi-bi mechanism.

Table 1: Kinetic Parameters for SRHEPT + A293D[a]

substrate	cosubstrate	k_{cat} (s^{-1})	K_m (mM)	k_{cat}/K_m ($\times 10^{-2}$ M^{-1} s^{-1})
Phe	α-KG	10 (0.6)	0.30 (0.03)	340 (50)
α-KG	Phe		0.48 (0.06)	210 (40)
Asp	α-KG	43 (3)	19 (2)	22 (2)
α-KG	Asp		2.6 (0.3)	160 (20)
Ala	α-KG	NS[b]	NS[b]	0.696 (0.002)

[a] Assays were performed in 200 mM TAPS at pH 8, 140 mM KCl, 20 μM PLP, and 150 μM NADH, with 68 nM SRHEPT + A293D. The concentrations of HO-HxoDH, MDH, or LDH were sufficiently high to ensure that the observed rates were independent of the concentration of coupling enzyme. The concentration of Phe varied from 0.02 to 0.90 mM, that of Asp from 0.5 to 40.0 mM, that of Ala from 1 to 160 mM, and that of α-KG from 0.05 to 10 mM except in the LDH-coupled assay, where it was held constant at 8 mM. Standard errors are in parentheses. [b] No saturation observed.

$$\frac{v}{[E_T]} = \frac{k_{cat}}{1 + \frac{K_m^{AA}}{[AA]} + \frac{K_m^{\alpha\text{-KG}}}{[\alpha\text{-KG}]}} \quad (1)$$

Dissociation Constants. The change in absorbance at 430 nm was measured as a function of Hca or maleate concentration, and data were fit to eq 2 with Kaleidagraph

$$A = A_0 - \frac{(A_0 - A_S)[L]}{K_D + [L]} \quad (2)$$

where A is the absorbance, A_0 is the absorbance in the absence of the inhibitor, and A_S is the absorbance at a saturating inhibitor concentration.

Table 2: Specificities of Wild-Type and Variant Aminotransferases[a]

variant	k_{cat}/K_m ($\times 10^{-2}$ M^{-1} s^{-1})			specificity[b]		
	Phe	Asp	Ala	Phe/Asp	Phe/Ala	Asp/Ala
eAATase	1.19[c]	900[d]	0.006[e] (0.0007)	0.001	180	130000
HEX	370[e] (20)	340[e] (50)	0.402[e] (0.005)	1.1	920	850
HEX + A293D	900[f] (20)	131[f] (7)	ND	6.9	ND	ND
SRHEPT	165[e] (7)	240[e] (2)	0.43[e] (0.01)	0.69	380	560
SRHEPT + A293D	340[g] (50)	22[g] (2)	0.696[g] (0.002)	15	490	32
eTATase	9600[h]	370[h]	0.0273[e] (0.0003)	26	350000	13000

[a] Standard errors are in parentheses. [b] Defined as the ratio of k_{cat}/K_m values. [c] From ref *1*. [d] From ref *2*. [e] From ref *11*. [f] From ref *30*. [g] From Table 1. [h] From ref *3*.

Crystallization. Crystals were grown at 19°C by the hanging-drop technique under the previously described conditions (*15*), with modifications. Drops (3 μL) containing 30 mg/mL purified enzyme in 20 mM potassium phosphate at pH 7.5, 10 μM PLP, 2 mM EDTA, and 0.5 mM DTT were mixed with 3 μL of reservoir solution (2% PEG 400, 200 mM *N*-methylmorpholine at pH 7.5, and 1.95−2.35 M ammonium sulfate). Enzyme−inhibitor complexes were obtained by cocrystallization with either maleate or Hca (20 mM).

Structural Analysis. All diffraction data were collected on beamline 8.3.1 at the Advanced Light Source at Lawrence Berkeley National Laboratory. Data were indexed, integrated, and scaled with HKL2000 (*16*). After subtraction of the ligands from the models, the structures were determined by molecular replacement with AMoRe (*17*). Ligand-free HEX [PDB entry 1AHE (*15*)] served as a starting model for ligand-free HEX + A293D, the HEX−Hca complex [PDB entry 1AHX (*15*)] for Hca-inhibited HEX + A293D, SRHEPT, and SRHEPT + A293D, and the wild-type eAATase−maleate complex [PDB entry 1ASM (*18*)] for maleate-inhibited SRHEPT. Manual model building was carried out with O (*19*), followed by refinement using REFMAC5 (*20*), a second round of model building, and TLS refinement (*20*). Structural overlays for analysis were made using LSQKAB by aligning large domain residues (46−329). Images were produced with PyMOL (DeLano Scientific, 2002).

RESULTS

Steady-State Kinetics. Steady-state kinetic parameters for the SRHEPT + A293D variant of eAATase are given in Table 1. No saturation was observed up to 160 mM alanine. The value of k_{cat}/K_m for phenylalanine is more than 2 orders of magnitude greater than that for alanine, and is 15-fold greater than that for aspartate. The K_m for aspartate is nearly 2 orders of magnitude greater than that for phenylalanine, and ~50 times greater than the intracellular concentration of aspartate in *E. coli* (*21*). The K_m values for α-KG and phenylalanine are close to their physiological concentrations at 0.48−2.6 and 0.30 mM, respectively (*21*, *22*).

The kinetics exhibited by variant and wild-type aminotransferases with aspartate, phenylalanine, and alanine are collected in Table 2. The ratio of k_{cat}/K_m values for phenylalanine versus aspartate for SRHEPT + A293D is 15000-fold greater than that for wild-type eAATase, and is nearly equal to that of wild-type eTATase. However, the k_{cat}/K_m^{Phe} of SRHEPT + A293D, although 2-fold greater than that of SRHEPT, is 1 order of magnitude less than that of wild-type eTATase.

Table 3: Dissociation Constants of Aminotransferase Complexes[a]

	[maleate] (mM)	[hydrocinnamate] (mM)
eAATase	19[b] (1)	>75[c]
HEX	0.44[b] (0.12)	0.12[b] (0.03)
HEX + A293D	170[d] (30)	0.090 (0.004)
SRHEPT	3.4 (0.3)	0.41 (0.03)
SRHEPT + A293D	≫20	0.6 (0.1)
eTATase	140[b] (10)	12[b] (1)

[a] Assays were performed with 20 μM enzyme in 200 mM TAPS at pH 8, 140 mM KCl, and 20 μM PLP. The concentration of Hca varied from 0 to 6 mM and that of maleate from 0 to 10 mM. Standard errors are in parentheses. [b] From ref *9*. [c] From ref *25*. [d] From ref *10*.

Dissociation Constants. Table 3 presents the K_D values for the wild-type and variant aminotransferase−inhibitor complexes with maleate and Hca. Affinity for Hca is significantly enhanced for every variant, compared to those of the wild-type aminotransferases. The K_D values for maleate are more variable; they remain high for the HEX + A293D and SRHEPT + A293D complexes, but are more than 40-fold lower in HEX and SRHEPT than in eTATase. The high affinity of HEX for dicarboxylic ligands is likely responsible for its inability to function *in vivo* (*10*).

Crystal Structures. Wild-type eAATase is active as a dimer. Each monomer has 396 residues with one pyridoxal 5′-phosphate (PLP), and consists of a large domain (residues 47−329), a small domain (residues 16−46 and 330−409), and a short dimerization arm (residues 5−15).[2] The active site is comprised of residues from both chains (Figure 1). These characteristics also hold true for the following determined mutant eAATase structures: the unliganded and Hca complex of HEX + A293D, the Hca and maleate complexes of SRHEPT, and the Hca complex of SRHEPT + A293D. Data collection, refinement, and structural statistics are given in Table 4. The mutant complexes were refined to 2.0, 1.9, 1.9, 1.9, and 2.3 Å resolution, respectively, and all *R*-factors and stereochemical parameters are as expected for structures at this resolution. The SRHEPT−maleate and SRHEPT + A293D−Hca complexes were found to be in the $P6_3$ space group, which is novel for aspartate aminotransferase and its variants. The asymmetric unit contains either a dimer or a monomer for the $P6_3$ or $C222_1$ structure presented here, respectively.

HEX + A293D. The introduction of the A293D substitution into HEX does not greatly alter the mode of Hca binding. The α-carboxylate group of Hca forms hydrogen bonds with Arg 386, and its phenyl ring extends into a hydrophobic cluster comprised of Trp 140, Ile 37, Ile 17, and Leu 18 (*15*). As shown in Figure 2, Asp 293 forms a salt bridge with Arg 292 in both the unliganded and Hca-inhibited

Table 4: Collection, Refinement, and Structure Data from X-ray Crystallography

	HEX + A293D (unliganded)	HEX + A293D−Hca complex	SRHEPT−Hca complex	SRHEPT−maleate complex	SRHEPT + A293D−Hca complex
Data Collection					
resolution (Å)	50−2.0	50−1.9	30−1.9	50−1.85	30−2.3
wavelength (Å)	1.12	1.12	1.12	1.12	1.12
space group	$C222_1$	$C222_1$	$C222_1$	$P6_3$	$P6_3$
unit cell dimensions (*a*, *b*, *c*) (Å)	85.71, 152.87, 79.12	83.79, 154.85, 77.92	83.42, 156.03, 77.87	140.14, 140.14, 81.08	151.38, 151.38, 79.72
I/σ (last shell)	23.5 (2.1)	26.2 (6.5)	25.0 (3.7)	30.5 (3.3)	28.6 (14.4)
R_{sym}[a] (last shell) (%)	0.055 (0.338)	0.043 (0.161)	0.047 (0.251)	0.050 (0.362)	0.059 (0.136)
completeness (last shell) (%)	99.0 (91.7)	94.6 (82.1)	99.7 (97.6)	99.9 (99.9)	96.6 (99.1)
no. of reflections	456075	286478	413471	894682	682720
no. of unique reflections	35904	38227	40208	77194	44493
Refinement					
molecular replacement search model PDB entry	1AHE (monomer)	1AHX (monomer)	1AHX (monomer)	1ASM (dimer)	1AHX (dimer)
resolution (Å)	30−2.0	30−1.9	30−1.9	30−1.85	30−2.3
no. of reflections	33481	36230	38178	73288	42219
no. of working reflections	31714	34302	36168	69412	39964
no. of free reflections (% total)	1767 (5.0)	1928 (5.1)	2010 (5.0)	3876 (5.0)	2255 (5.1)
R_{work}[b] (last shell) (%)	17.78 (23.4)	17.34 (17.6)	18.11 (19.4)	19.41 (21.4)	18.48 (21.0)
R_{free}[b] (last shell) (%)	20.21 (25.1)	19.69 (21.9)	20.14 (21.6)	22.67 (29.0)	23.15 (26.2)
Structure and Stereochemistry					
no. of atoms	3268	3330	3241	6463	6329
protein	3074	3074	3067	6134	6140
water	174	230	148	283	137
PLP	15	15	15	30	30
inhibitor	5 (SO_4)	11 (Hca)	11 (Hca)	16 (maleate)	22 (Hca)
rmsd for bond lengths (Å)	0.011	0.010	0.010	0.012	0.014
rmsd for bond angles (deg)	1.31	1.17	1.27	1.40	1.51

[a] $R_{sym} = \sum\sum_j |I_j - \langle I \rangle| / \sum I_j$, where I_j is the intensity measurement for reflection j and $\langle I \rangle$ is the mean intensity for multiply recorded reflections. [b] $R_{work,free} = \sum ||F_{obs}| - |F_{calc}|| / |F_{obs}|$, where the working and free *R*-factors are calculated from the corresponding reflection sets. The free reflections were set aside throughout refinement.

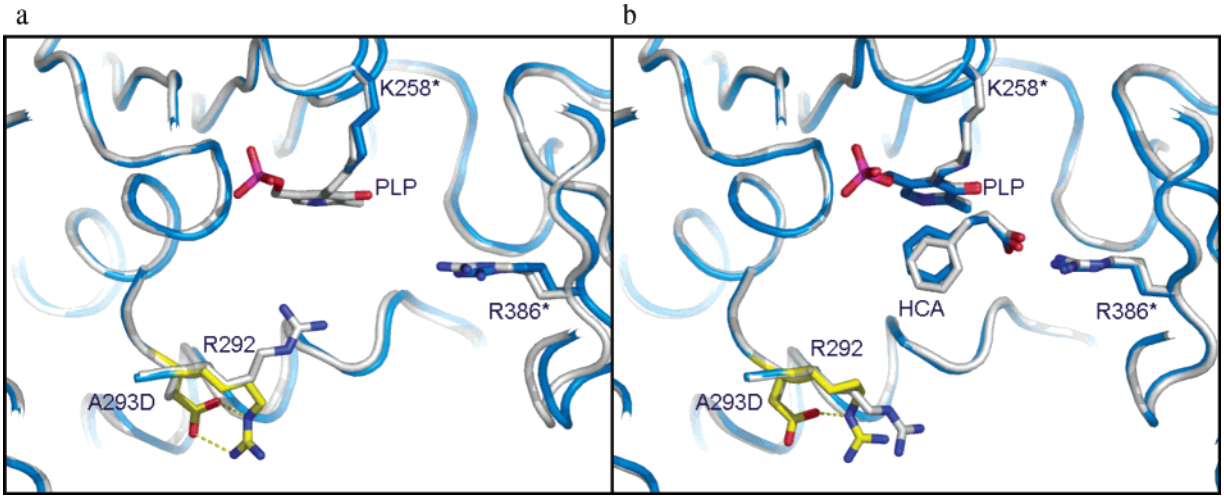

FIGURE 2: Position of Arg 292 in HEX + A293D (blue) and HEX (gray). Arg 292, Asp 293, and the hydrogen bond between them are highlighted in yellow in the HEX + A293D structure. An asterisk denotes that the residue is contributed by the other subunit. (a) An overlay of the unliganded complexes of the two enzymes shows that while Arg 292 occupies the active site in HEX, it is pulled down by interactions with Asp 293 in HEX + A293D. The carboxylate oxygens of Asp 293 form two hydrogen bonds of 2.8 and 3.0 Å with N_ϵ and N_η of Arg 292, respectively. The sulfate molecule occupying the active site is not shown. (b) Arg 292 swings down to accommodate the large, nonpolar inhibitor in the Hca complexes of both variants; however, Arg 292 is slightly farther from the active site in the HEX + A293D structure than it is in HEX.

structures of HEX + A293D, holding Arg 292 away from the active site. The hydrogen bonds that are observed between Arg 292 and Asp 15 (not shown) in the unliganded HEX complex are disrupted by Asp 293. These changes induced by the mutation at 293 lead to an extra degree of flexibility for the small domain residues of HEX + A293D, which move up to 3 Å upon association with Hca (Figure 3).

SRHEPT and SRHEPT + A293D. Attempts to crystallize the unliganded forms of SRHEPT and SRHEPT + A293D were unsuccessful. However, liganded complexes were crystallized and their structures determined. SRHEPT as-

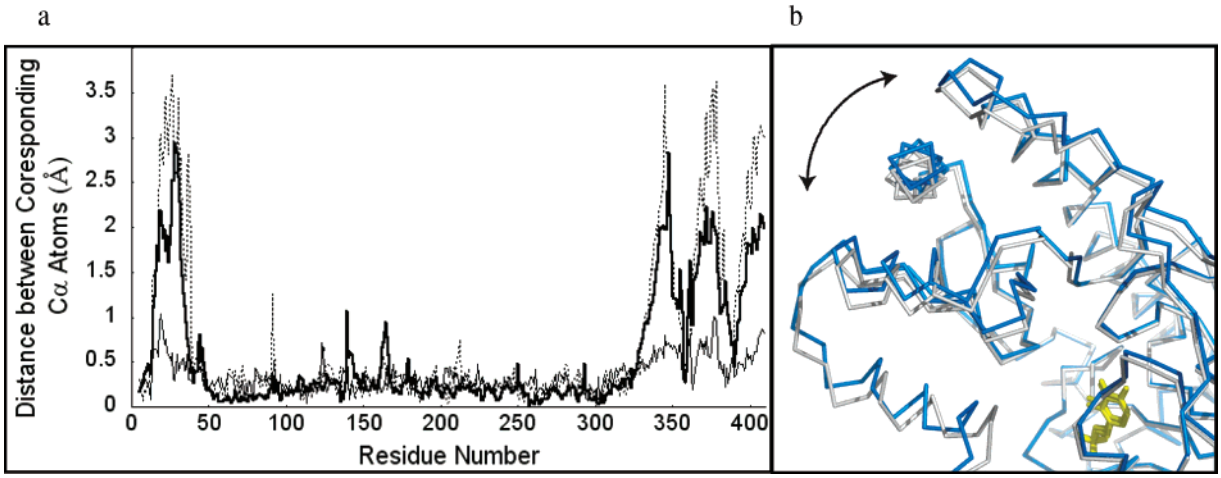

FIGURE 3: Small domain (residues 16−47 and 326−409) movement accompanies complex formation. (a) The dotted line shows movement of C_α atoms between the closed and half-open conformations of wild-type eAATase. The solid thin and thick lines show the distance between corresponding C_α atoms of the unliganded and Hca complexes of HEX and HEX + A293D, respectively. Upon association of Hca, HEX remains closed while HEX + A293D adopts a new conformation intermediate between the closed and half-open states; there is significant movement of HEX + A293D C_α atoms in the small domain that reach nearly 3 Å. (b) One of the small subunits of unliganded HEX (gray) and HEX + A293D (blue) with bound PLP (yellow). While the backbones of the large domains for both structures are almost exactly superimposable (not shown), those of the small domains are not.

sociates with Hca and maleate in the same manner as in HEX complexes (*15*). Comparison of the maleate and Hca complexes of SRHEPT provides additional support for the substrate-recognition function of Arg 292; while the guanidine side chain points away from the active site in the Hca complex, it makes a salt bridge with the carboxylate group of bound maleate. Upon introduction of the A293D substitution into SRHEPT, N_ϵ of Arg 292 swings 2.5 Å away from the active site toward the Asp 293 side chain, and forms a new hydrogen bond with the Asp 293 carboxylate.

DISCUSSION

Substrate Specificity of SRHEPT + A293D. Adaptation of an enzyme for targeting a new substrate in directed evolution is generally achieved by specificity relaxation (*23*, *24*). The introduction of the A293D substitution does not enhance the selectivity of aspartate over alanine in SRHEPT (Table 2), but increases the ratio of k_{cat}/K_m^{Phe} to k_{cat}/K_m^{Asp} in both HEX and SRHEPT through a reduction in k_{cat}/K_m^{Asp}.

Introduction of the A293D Substitution in Two Contexts. The effects of the added A293D mutation can be appreciated by comparing the properties of SRHEPT + A293D to those of SRHEPT, and those of HEX + A293D to those of HEX. The affinity for aromatic substrates over dicarboxylic ones is enhanced in both cases, but to different degrees. The A293D mutation increases $K_D^{maleate}$ by 380-fold in HEX and ≥10-fold in SRHEPT (Table 3). There is little effect on K_D^{Hca} upon introduction of the A293D substitution in either case. Thus, the introduction of the A293D substitution enhances selectivity for Hca over maleate.

Kinetic data presented in Table 2 extend these results. SRHEPT + A293D has a 2-fold greater k_{cat}/K_m^{Phe} than SRHEPT, and an almost 11-fold lesser k_{cat}/K_m^{Asp}. Thus, introduction of the A293D mutation enhances specificity for phenylalanine over aspartate by more than 21-fold. Adding A293D to HEX more than doubles k_{cat}/K_m^{Phe}, an effect similar to that realized by the corresponding addition to SRHEPT. However, k_{cat}/K_m^{Asp} decreases only 2-fold. The effect of the A293D mutation is to increase the specificity for phenylalanine over aspartate by only 6-fold in the context of HEX. This is 4 times lower than the corresponding change in SRHEPT. It follows that the effect of this single substitution not only can be added to the effects of other mutations in the enzyme but also is context-dependent.

Comparative Quantitative Analysis of the Introduction of the A293D Substitution of HEX and SRHEPT. The terms *I* (impact) and *C* (context dependence) were introduced to quantitate substitutions in the analysis of chimeras (*1*, *25*). They are defined in eqs 3 and 4:

$$I_{chimera} = \Delta\Delta G_{S_{A\rightarrow B}} - \Delta\Delta G_{S_{B\rightarrow A}} \quad (3)$$

$$C_{chimera} = \Delta\Delta G_{S_{A\rightarrow B}} + \Delta\Delta G_{S_{B\rightarrow A}} \quad (4)$$

where the $S_{A\rightarrow B}$ and $S_{B\rightarrow A}$ subscripts refer to the change in free energy effects observed on an addressable parameter in the forward chimeras and retrochimeras, respectively. Both *I* and *C* are necessary to distinguish the trivial case in which $I \cong C \cong 0$ (*1*, *25*).

I and *C* values can be extended to provide a quantitative understanding of the effects of introduction of a common replacement into two or more different protein scaffolds. They are applied here to the A293D replacement in HEX and SRHEPT. Equations 3 and 4 need to be modified for this purpose because the replacement is the same, while in chimeras, the second replacement reverses the first.

$$I_{replacement} = \Delta\Delta G_{S_{A\rightarrow A+X}} + \Delta\Delta G_{S_{B\rightarrow B+X}} \quad (5)$$

$$C_{replacement} = \Delta\Delta G_{S_{A\rightarrow A+X}} - \Delta\Delta G_{S_{B\rightarrow B+X}} \quad (6)$$

In our application of eqs 5 and 6, X is the common replacement, A293D, and A and B are the scaffolds, HEX and SRHEPT. Substitutions that are independent of the accepting platform have a $C_{replacement}$ of 0, while the corresponding *I* value measures the magnitude of the effect on the addressed parameter.

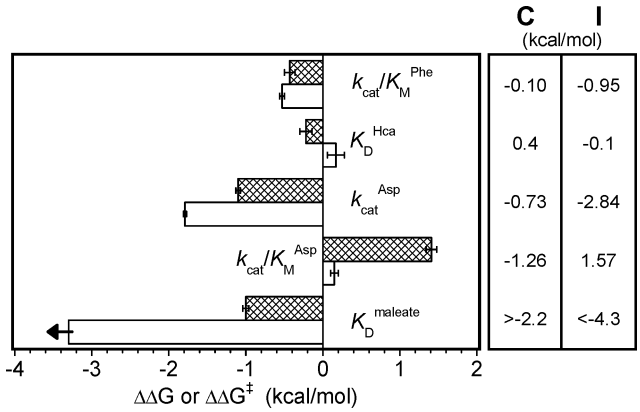

FIGURE 4: Impact and context dependence of the A293D substitution in two scaffolds. The free energy or transition-state free energy for each of four related eAATase variants (HEX, HEX + A293D, SRHEPT, and SRHEPT + A293D) was calculated for the kinetic and binding parameters of aromatic and dicarboxylic ligands. Plots are shown for the $\Delta\Delta G$ or $\Delta\Delta G^{\ddagger}$ for HEX + A293D compared to its parent scaffold HEX (white bars) and SRHEPT + A293D compared to its parent SRHEPT (hatched bars). The impact of A293D on ligand binding and substrate specificity is the sum of the $\Delta\Delta G$ values of SRHEPT and HEX, while the context dependence of this replacement is calculated by subtracting the $\Delta\Delta G$ of SRHEPT from that of HEX. The A293D substitution has a small impact on specificity for aromatic ligands, and a large impact on specificity of dicarboxylic ligands. Likewise, the context dependence of this replacement is negligible for aromatic compounds and moderate for dicarboxylic ligands.

Figure 4 illustrates that A293D has a large impact and moderate context dependence with respect to dicarboxylic ligands, and that both the impact and context dependence are insignificant with respect to aromatic ligands. Therefore, A293D selectively modulates interaction with dicarboxylic ligands. The similar magnitudes and opposite signs of *I* and *C* for k_{cat}/K_m^{Asp} signify that the A293D substitution plays a larger role in aspartate specificity for one scaffold compared to the other. The negative value of *C* for k_{cat}/K_m^{Asp} reveals that the effect is larger in SRHEPT.

Structural Effects of the A293D Replacement. The mechanism through which the A293D mutation affects HEX substrate specificity manifests in two ways: (1) through repositioning of the Arg 292 side chain and (2) through small domain movement.

Interaction of wild-type eAATase with dicarboxylic substrates is largely achieved through salt bridge contacts with the guanidine side chains of Arg 292 and Arg 386, which are pointed into the active site; this is termed the "up" conformation of the Arg 292 arm. Arg 292 in HEX also exists in the up conformation (Figure 2a), as well as in a "down" conformation that has never been observed in wild-type eAATase. In the latter form, depicted in Figure 2b, Arg 292 swings away from the active site to accommodate larger aromatic substrates. Introduction of the A293D mutation into HEX relieves dicarboxylic acid hyperaffinity because Arg 292 is maintained in the down conformation through interaction with Asp 293 (Figure 2a,b). This new orientation disfavors association with dicarboxylate ligands.

The eAATase reaction is catalyzed through an induced fit mechanism, where the small domain pivots away from the large domain prior to product release (*18*, *26*). Since the active site is at the interface of the large and small domains, the change in conformation from the "closed" to "half-open" form allows diffusion of molecules into and out of the active site. However, crystal structures of HEX show that this variant does not change conformation, but remains closed regardless of whether ligand is bound (*15*). Four of the engineered substitutions in HEX (V39L, K41Y, T47I, and N69L) extend a hydrophobic patch that includes the side chains of Tyr 263, Trp 140, Tyr 70, Ile 73, Ile 37, Leu 18, and Ile 17 (*27*). The nonpolar cluster stabilizes the closed conformation (*15*). It was argued that the failure of HEX to function as an aromatic aminotransferase *in vivo* is due to product inhibition from tightly bound dicarboxylic acids, which results from the inflexibility of the small domain (*10*). These data provide structural verification for that conjecture.

Introduction of A293D results in a novel intermediate conformation between the half-open and closed states that may decrease the energetic barrier for product release compared to that extant for the HEX complexes. Whereas small domain residues shift more than 3.5 Å between the half-open and closed conformations of wild-type eAATase upon substrate association (*18*), they do not move significantly in HEX, which is stabilized in the closed conformation. Introduction of the A293D substitution partially restores domain flexibility such that corresponding residues in HEX + A293D move up to 3 Å upon substrate binding (Figure 3). Furthermore, the direction of movement of small domain residues between the closed and open forms is different than what has been observed in eAATase. The small domain of HEX + A293D opens along a vector that is approximately 40° different from that of wild-type eAATase.

The A293D mutation promotes domain opening by altering interactions between key residues in the enzyme. Specifically, Arg 292 forms hydrogen bonds with Asp 15 and Ser 296 in unliganded structures of eAATase and HEX, but these bonds are broken in HEX + A293D. Similarly, Arg 292 forms a hydrogen bond with Asn 142 in Hca-bound HEX; however, the bond is broken in HEX + A293D, and Arg 292 makes a new hydrogen bond with Asp 15. In both cases, Arg 292 makes new hydrogen bonds with Asp 293 (Figure 2).

Structural Effects of SRHEPT and SRHEPT + A293D Replacements. Residues in the N-terminal region interact with the large domain of the other subunit. The loss in activity for aromatic substrates upon substitution of the flexible eTATase N-terminal arm with corresponding eAATase residues suggested that they constitute an important specificity determinant (*28*). High-resolution crystal structures of *Paracoccus denitrificans* TATase supported this conclusion by implicating flexibility of residues 15 and 16 in ligand recognition (*29*).

Substitution of a proline at position 13 with threonine in SRHEPT and SRHEPT + A293D increases the freedom of motion in this region, leading to enhanced aromatic substrate recognition with respect to wild-type eAATase. Mobility is likely further improved when a hydrogen bond between the main chain nitrogen of residue 12 and Ser 285 O_γ is broken due to the evolved S285G mutation. These two substitutions permit greater movement of the N-terminal residues upon introduction of the A293D mutation into SRHEPT than when the mutation is introduced into HEX (Figure 5). It is unclear what role, if any, the A12T mutation plays in SRHEPT and SRHEPT + A293D. Although all replacements in SRHEPT were chosen on the basis of the frequency with which they appeared in evolved variants, only the P13T mutation was

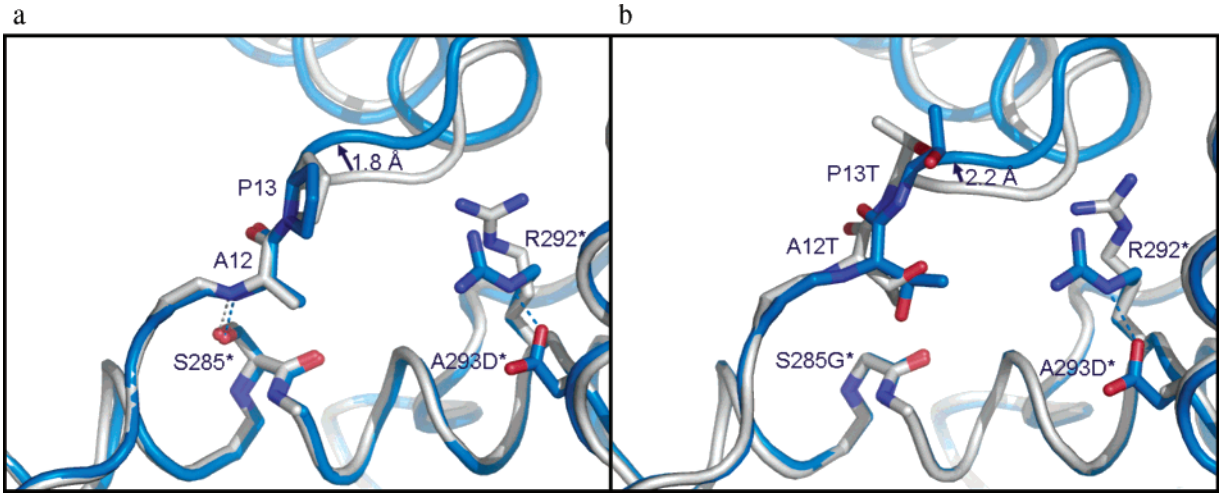

FIGURE 5: Flexibility of the N-terminus. The Hca complexes of HEX (gray) and HEX + A293D (blue) are shown in panel a and those of SRHEPT (gray) and SRHEPT + A293D (blue) in panel b. A dashed line indicates selected hydrogen bonds, and an asterisk denotes that the residue is contributed by the other subunit. The active site and the inhibitor are out of view to the top right. The movement in the N-terminus of the SRHEPT structure due to the added A293D mutation is greater than that of HEX. For example, the C_α atom of residue 14 moves 2.2 Å upon addition of the A293D substitution in SRHEPT (direction indicated by an arrow), but only 1.8 Å in the HEX scaffold. There are three amino acid substitutions in this region in SRHEPT (A12T, P13T, and S285G) that are absent in HEX.

found in all 12 of the sequenced clones, whereas S285G and A12T were each found in only three (*11*). Thus, the P13T substitution is likely the most important factor in conferring aromatic aminotransferase ability in SRHEPT, and contributes most to the flexibility of the N-terminal arm. The S285G and A12T mutations likely augment the effect, but are less critical.

The G261A replacement is located at the far end of the hydrophobic patch next to Tyr 263. It extends this patch and likely contributes the same function as the V39L, K41Y, T47I, and N69L mutations did in HEX, producing a more hydrophobic active site to promote binding of aromatic ligands and stabilizing the closed conformation to facilitate tight binding of both aromatic and dicarboxylic ligands.

The N34D mutation in SRHEPT is located near the opposite end of the active site. In the unliganded eAATase structure, the side chain of Asn 34 is 3.0 Å from the backbone nitrogen of Gly 36. One subunit maintains this hydrogen bond in the maleate complex, but the other does not. That hydrogen bond is present in both subunits of inhibited SRHEPT and SRHEPT + A293D. The result is that the carbonyl oxygen of Gly 36 is held 3.0−3.2 Å from N_ϵ of Arg 386 in SRHEPT and SRHEPT + A293D, but this hydrogen bond occurs in only one subunit of the maleate-inhibited wild-type eAATase structure. In all wild-type and variant eAATases, Arg 386 forms a salt bridge with the carboxylate of dicarboxylic and aromatic ligands. The N34D mutation may serve to enhance ligand recognition by Arg 386 through a strengthened hydrogen bond with Gly 36.

The T109S and N297S substitutions in HEX were evaluated previously (*15*, *25*), and their roles in SRHEPT and SRHEPT + A293D are expected to be similar. The T109S mutation extends a contact surface for the substrate phenyl ring by rearranging a hydrogen bond network, while the N297S replacement serves to pull a water molecule away from the active site that would otherwise interfere with aromatic ligand association. Both modifications specifically tailor the active site to accommodate aromatic ligands.

Concluding Remarks. Why do naturally occurring TATases and the directly evolved enzymes survive *in vivo* while HEX does not? Two factors contribute to tight binding of dicarboxylic products and substrates: the up conformation of the Arg 292 arm and the closed domain configuration in the unliganded form. Tight ligand binding results from favoring both of these conformations, and relaxation of either factor reduces affinity. HEX has both factors, but it is likely that SRHEPT adopts a more open conformation as it contains only a single mutation at the domain interface. The introduction of the A293D mutation further reduces dicarboxylic acid specificity selectively by removing the important salt bridge between Arg 292 and the ligand, and relaxes the closed conformation, thus relieving the product inhibition exhibited by HEX.

ACKNOWLEDGMENT

We thank Dr. James Holton for assistance in maintaining Advanced Light Source beamline 8.3.1 and Dr. Steven Rothman for valuable advice.

REFERENCES

1. Luong, T. N., and Kirsch, J. F. (2001) A general method for the quantitative analysis of functional chimeras: Applications from site-directed mutagenesis and macromolecular association, *Protein Sci. 10*, 581−591.
2. Gloss, L. M., and Kirsch, J. F. (1995) Decreasing the basicity of the active site base, Lys258, of *Escherichia coli* aspartate aminotransferase by replacement with gamma thialysine, *Biochemistry 34*, 3990−3998.
3. Hayashi, H., Inoue, K., Nagata, T., Kuramitsu, S., and Kagamiyama, H. (1993) *Escherichia coli* aromatic amino acid aminotransferase: Characterization and comparison with aspartate aminotransferase, *Biochemistry 32*, 12229−12239.
4. Penning, T. M., and Jez, J. M. (2001) Enzyme redesign, *Chem. Rev. 101*, 3027−3046.
5. Joerger, A. C., Mayer, S., and Fersht, A. R. (2003) Mimicking natural evolution *in vitro*: an *N*-acetylneuraminate lyase mutant with an increased dihydrodipicolinate synthase activity, *Proc. Natl. Acad. Sci. U.S.A. 100*, 5694−5699.
6. Ulrich, S. M., Kenski, D. M., and Shokat, K. M. (2003) Engineering a "methionine clamp" into Src family kinases enhances specificity toward unnatural ATP analogues, *Biochemistry 42*, 7915−7921.

7. Kortemme, T., Joachimiak, L. A., Bullock, A. N., Schuler, A. D., Stoddard, B. L., and Baker, D. (2004) Computational redesign of protein−protein interaction specificity, *Nat. Struct. Mol. Biol. 11*, 371−379.
8. Seebeck, F. P., and Hilvert, D. (2003) Conversion of a PLP-dependent racemase into an aldolase by a single active site mutation, *J. Am. Chem. Soc. 125*, 10158−10159.
9. Onuffer, J. J., and Kirsch, J. F. (1995) Redesign of the substrate specificity of *Escherichia coli* aspartate aminotransferase to that of *Escherichia coli* tyrosine aminotransferase by homology modeling and site-directed mutagenesis, *Protein Sci. 4*, 1750−1757.
10. Rothman, S. C., Voorhies, M., and Kirsch, J. F. (2004) Directed evolution relieves product inhibition and confers *in vivo* function to a rationally designed tyrosine aminotransferase, *Protein Sci. 13*, 763−772.
11. Rothman, S. C., and Kirsch, J. F. (2003) How does an enzyme evolved *in vitro* compare to naturally occurring homologs possessing the targeted function? Tyrosine aminotransferase from aspartate aminotransferase, *J. Mol. Biol. 327*, 593−608.
12. Herold, M., and Kirschner, K. (1990) Reversible dissociation and unfolding of aspartate aminotransferase from *Escherichia coli:* Characterization of a monomeric intermediate, *Biochemistry 29*, 1907−1913.
13. Goldberg, J. M., and Kirsch, J. F. (1996) The reaction catalyzed by *Escherichia coli* aspartate aminotransferase has multiple partially rate-determining steps, while that catalyzed by the Y225F mutant is dominated by ketimine hydrolysis, *Biochemistry 35*, 5280−5291.
14. Luong, T. N., and Kirsch, J. F. (1997) A continuous coupled spectrophotometric assay for tyrosine aminotransferase activity with aromatic and other nonpolar amino acids, *Anal. Biochem. 253*, 46−49.
15. Malashkevich, V. N., Onuffer, J. J., Kirsch, J. F., and Jansonius, J. N. (1995) Alternating arginine-modulated substrate specificity in an engineered tyrosine aminotransferase, *Nat. Struct. Biol. 2*, 548−553.
16. Otwinowski, Z., and Minor, W. (1997) Processing of X-ray diffraction data collected in oscillation mode, *Methods Enzymol. 276*, 307−326.
17. Navaza, J. (2001) Implementation of molecular replacement in AMoRe, *Acta Crystallogr. D57*, 1367−1372.
18. Jager, J., Moser, M., Sauder, U., and Jansonius, J. N. (1994) Crystal structures of *Escherichia coli* aspartate aminotransferase in two conformations. Comparison of an unliganded open and two liganded closed forms, *J. Mol. Biol. 239*, 285−305.
19. Jones, T. A., Zou, J. Y., Cowan, S. W., and Kjeldgaard, M. (1991) Improved methods for building protein models in electron-density maps and the location of errors in these models, *Acta Crystallogr. A47*, 110−119.
20. Winn, M. D., Isupov, M. N., and Murshudov, G. N. (2001) Use of TLS parameters to model anisotropic displacements in macromolecular refinement, *Acta Crystallogr. D57*, 122−133.
21. Lowry, O. H., Carter, J., Ward, J. B., and Glaser, L. (1971) The effect of carbon and nitrogen sources on the level of metabolic intermediates in *Escherichia coli*, *J. Biol. Chem. 246*, 6511−6521.
22. Raunio, R., and Rosenqvist, H. (1970) Amino acid pool of *Escherichia coli* during the different phases of growth, *Acta Chem. Scand. 24*, 2737−2744.
23. Matsumura, I., and Ellington, A. D. (2001) *In vitro* evolution of β-glucuronidase into a β-galactosidase proceeds through non-specific intermediates, *J. Mol. Biol. 305*, 331−339.
24. Yano, T., Oue, S., and Kagamiyama, H. (1998) Directed evolution of an aspartate aminotransferase with new substrate specificities, *Proc. Natl. Acad. Sci. U.S.A. 95*, 5511−5515.
25. Shaffer, W. A., Luong, T. N., Rothman, S. C., and Kirsch, J. F. (2002) Quantitative chimeric analysis of six specificity determinants that differentiate *Escherichia coli* aspartate from tyrosine aminotransferase, *Protein Sci. 11*, 2848−2859.
26. McPhalen, C. A., Vincent, M. G., Picot, D., Jansonius, J. N., Lesk, A. M., and Chothia, C. (1992) Domain closure in mitochondrial aspartate aminotransferase, *J. Mol. Biol. 227*, 197−213.
27. Jager, J., Pauptit, R. A., Sauder, U., and Jansonius, J. N. (1994) Three-dimensional structure of a mutant *E. coli* aspartate aminotransferase with increased enzymic activity, *Protein Eng. 7*, 605−612.
28. Kawaguchi, S., Nobe, Y., Yasuoka, J., Wakamiya, T., Kusumoto, S., and Kuramitsu, S. (1997) Enzyme flexibility: A new concept in recognition of hydrophobic substrates, *J. Biochem. 122*, 55−63.
29. Okamoto, A., Ishii, S., Hirotsu, K., and Kagamiyama, H. (1999) The active site of *Paracoccus denitrificans* aromatic amino acid aminotransferase has contrary properties: flexibility and rigidity, *Biochemistry 38*, 1176−1184.
30. Rothman, S. C. (2003) Ph.D. Thesis, University of California, Berkeley, CA.

BI0487544